DOI: 10.1002/ejic.201001284

Facile Solvothermal Synthesis of Uniform Iron Selenide Nanoplates

Liqiao Chen,[a,b] Xianfeng Yang,[a] Xionghui Fu,[a] Chaomin Wang,[a] Chaolun Liang,[a] and Mingmei Wu*[a]

Keywords: Iron / Selenium / Nanostructures / Solvothermal synthesis

Nanostructures of $FeSe_x$ with a tetragonal PbO-type phase have been grown through a new and simple solvothermal route. By adding polyvinyl pyrrolidone (PVP) as a controlling reagent, the products change from nanoflowers to regular square nanoplates. Both the phase and structure are identified by powder X-ray diffraction and electron microscopy. The square nanoplates are revealed to be enclosed by two larger (001) planes and four equivalent smaller {100} side surfaces. The choice of the solvent is also important for the successful synthesis of the tetragonal PbO-type phase. This growth approach is not only facile and mild, but is also more advantageous for obtaining uniform $FeSe_x$ nanocrystals over other methods reported previously.

Introduction

Tetragonal PbO-type $FeSe_x$ represents an interesting kind of material, which has been proven to have potential in many fields because of its magnetic,[1–3] electrochemical,[4] optical, and electrical properties.[5,6] Significantly, the discovery of its superconductivity[7] has generated more and more attention to the preparation, structure, and properties of the family of $FeSe_x$ materials with tunable composition.[8–14] Experimental results show that the superconductivity and other physical properties are highly orientation- and thickness-dependent.[15] Samples with a specified shape are very necessary for scientists to study shape-related $FeSe_x$ properties.[16] Therefore, it is of significant importance to synthesize phase-pure PbO-type $FeSe_x$ samples with a specified shape and with uniform structure.

Many groups have been challenged by the controlled growth of tetragonal-phase β-$FeSe_x$, and, the samples with regular shape and size were achieved with difficultly.[17,18] To date, most products have been prepared at high temperatures by a solid-state reaction,[19–21] a flux growth method,[22,23] and by vapor self transport.[24] These routes successfully fabricate samples with different composition, but the particle sizes of the as-obtained samples are usually microsized and the shapes could not be controlled. FeSe/C core-shell nanofibers were synthesized by reaction of $Fe(CO)_5$ with Se powders in a closed reactor at 700 °C,[25] and stoichiometric β-FeSe superconductors with size of ca. 60 nm were prepared by mechanical alloying (MA) from elemental powders of iron and selenium (1:1) and subsequent annealing at ca. 400 °C,[26] but the difficulty in controlling the size distribution and shape was not overcome. Solution-based chemical routes can allow monodisperse and shape-controllable crystal growth under facile conditions. Previously, orthorhombic $FeSe_2$ nano- and microcrystals have been grown by solvothermal routes, but only an non-tetragonal phase was isolated.[27] Recently, predominantly two-dimensional multiple-crystal nanosheets were reported by Schaak et al., who adopted $Fe(CO)_5$ as the iron source and TOPO as the solvent.[17] We also reported a wet chemical route to more uniform quadrangle β-$FeSe_x$ nanoplates using oleylamine as solvent; however, in these methods, the processes are still sophisticated and costly. In addition, only very thin flakes (about 10 nm) can be obtained by these growth routes, which limits the study of the important dimension-dependent properties of β-$FeSe_x$. Very recently, a microwave-assisted method was used to prepare flowerlike β-FeSe microstructures.[18] Therefore, it is quite necessary to explore a new approach to synthesize uniform nanostructured β-FeSe. Herein, we present a new and facile solvothermal synthesis to obtain uniform square nanoplates of tetragonal β-$FeSe_x$, in which iron chloride ($FeCl_2$) and Se powders were used as the source and glycol as the solvent.

[a] State Key Laboratory of Optoelectronic Materials and Technology/MOE Key Laboratory of Bioinorganic and Synthetic Chemistry, School of Chemistry and Chemical Engineering, Instrumental Analysis and Research Centre, Sun Yat-Sen (Zhongshan) University, Guangzhou 510275, P. R. China
Fax: +86-20-84111038
E-mail: ceswmm@mail.sysu.edu.cn
[b] State Key Lab of Advanced Technology for Comprehensive Utilization of Platinum Metals, Kunming Institute of Precious Metals, Kunming 650106, P. R. China

Results and Discussion

Characterization of Structure and Composition

The product generated from the reaction of iron chloride ($FeCl_2$) and selenium powder was analyzed by using a powder X-ray diffraction (pXRD) technique. A pXRD pattern

shown in Figure 1 matches well with the JCPDS card No.85–0735 for tetragonal $FeSe_x$ with a = b = 3.765 and c = 5.518, which suggests that a PbO-type $FeSe_x$ ($P4/nmm$) structure is present in the product.[7] The complete absence of additional diffractions because of impurity phases indicates that phase-pure tetragonal $FeSe_x$ could be obtained by using such a simple solvothermal synthesis.

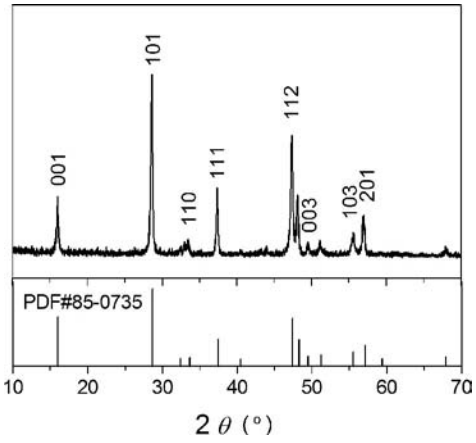

Figure 1. Powder X-ray diffraction pattern of a typical product after grinding. Information from a standard JCPDS card No. 85–0735 is given on the bottom.

The structures of the as-prepared product were characterized by SEM (Figure 2a), which shows that all of the products were crystallized in square plates with an edge length of about 1.0–2.0 μm and thickness of about 150 nm (Figure 2a, inset). These nanoplates were also characterized by TEM and selective area electron diffraction (SAED) (Figure 2b), which was taken from one part of the flake highlighted in the white square. The zone axis of the nanoplate is along the [001] direction when it is lying horizontally, which reveals that a nanoplate is enclosed by two crystallographically equivalent {001} and four equivalent {100} lattice planes as larger top-down and smaller side surfaces, respectively. This orientation growth of the nanoplates can be further confirmed by another pXRD pattern (Figure 2c), for which the sample without grinding was prepared by an elaborate precipitation on Si substrates to ensure that most of the nanoplates lie along the a–b plane. The significantly improved intensity of (00X) diffraction peaks in the pXRD confirms a preferred orientation of the as-synthesized crystals, consistent with the results from TEM images and related SAED (Figure 2b). The highly retarded growth along the c direction and the enhanced growth along a–b planes is rationalized by the inherent layer crystal structure of $FeSe_x$, as shown in Figure 2d in which covalently bonded Fe and Se slabs vertically stack together along the c axis through van der Waals forces (Figure 2d). This structure is similar to that prepared by a different synthetic route in our previous work.[28] Obviously, the reaction strategy presented in this paper is much more economic and facile. Furthermore, the sample with a 140-nm thickness along the c direction, which is thought as critical size,[15] would be of great importance to study its physical performance.

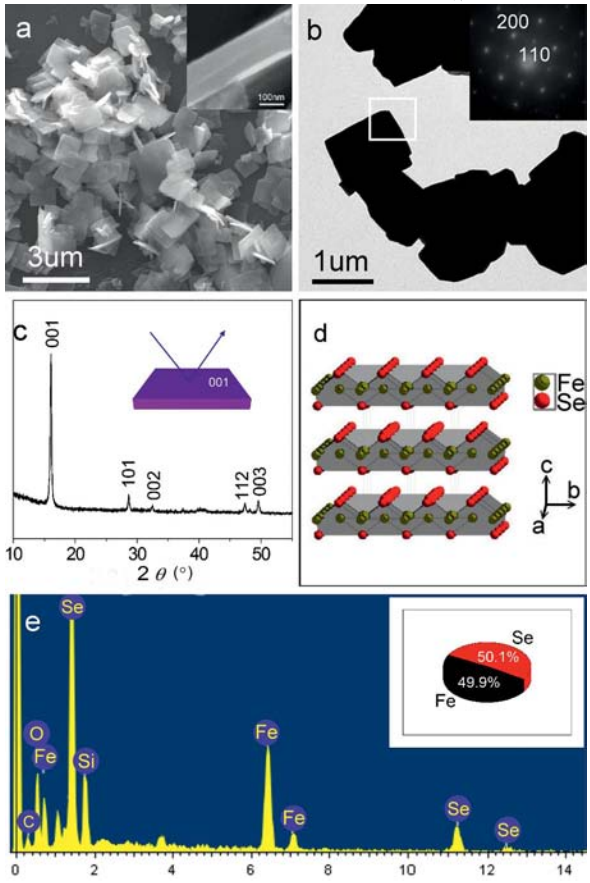

Figure 2. (a) SEM images of some nanoplates, (b) TEM images with a SAED pattern (inset), (c) powder X-ray diffraction pattern of the sample lying on a Si wafer substrate, (d) layered structure model, and (e) related EDS profile with resultant atomic percent $FeSe_x$.

The relative ratio of the composition of Fe and Se in the nanoplate was determined by using an energy dispersive X-ray spectroscopy (EDS) technique from the whole stack of the sample in the SEM image (Figure 2e). The atomic percentages of Fe and Se are 49.9 and 50.1%, respectively. That is, the chemical formula corresponds to $FeSe_{1.003}$. When the relative ratio was determined by using inductively coupled plasma atomic emission spectrometry (ICP) technique, the atomic percentages of Fe and Se are 53.1 and 46.9%, respectively. The chemical formula is calculated to be $FeSe_{0.89}$. Both of the results indicate the product $FeSe_x$ is nearly chemically stoichiometric. Previously, the $FeSe_x$ product was isolated by using $Fe(CO)_5$ as the iron source.[17] Herein, the economic and safe $FeCl_2$ and Se powders were used as the sources, respectively, and the synthesis approach is much more facile and economic.

The Role of PVP: The Control of the Nanostructures

PVP has successfully been used in the synthesis of nanomaterials as an important surfactant.[29,30] In the absence of PVP, poorly defined products were harvested (Figure 3). In

comparison with the product, which was synthesized in the presence of 0.03 g PVP (Figure 2a), these plates appear to be larger and thicker with more irregular shapes. Interestingly, during the mixing of the starting materials, if magnetic stirring was not introduced, flowerlike $FeSe_x$ aggregates grew in the absence of PVP. The size of each flowerlike aggregate is about 10–20 μm, which was built by the assembly of $FeSe_x$ nanosheets with a thickness of ca. 150 nm (Figure 4a). However, with the addition of trace amounts of PVP, such as 0.01 g in the typical reaction setup, the nanoplates do not appear as flowerlike aggregates, but separate from each other (Figure 4b). With further addition of PVP, the nanoplates tend to be more uniform and regular. Such an observation clearly indicates that PVP has a great affect on the control of $FeSe_x$ growth and promotes the dispersion of $FeSe_x$ crystals when PVP molecules are adsorbed on the $FeSe_x$ crystal surfaces. During the aging of the FeSe crystals, the formed crystal surfaces must be stabilized through chemical interactions with the oxygen (and/or nitrogen) atoms of the pyrrolidone groups of PVP,[31] and hence agglomeration among the formed crystals is avoided. However, in the absence of PVP, the dispersion of the particles must be performed through magnetic stirring. With increasing the amount of PVP, the square nanoplates with four {100} sides become more apparent, which implies that it is likely that PVP is adsorbed on the {100} surfaces. This confirms the study by Xia et al., which shows that PVP binds more strongly to {100} than to the {111} facets of Ag and can thereby reduce the growth rate along the [100] direction.[32] The pXRD pattern (Figure 5) confirms that all of these products crystallize in the phase-pure tetragonal PbO-type structure.

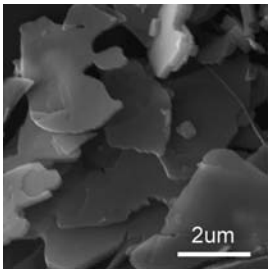

Figure 3. SEM image of the product grown from the starting mixture in the absence of PVP.

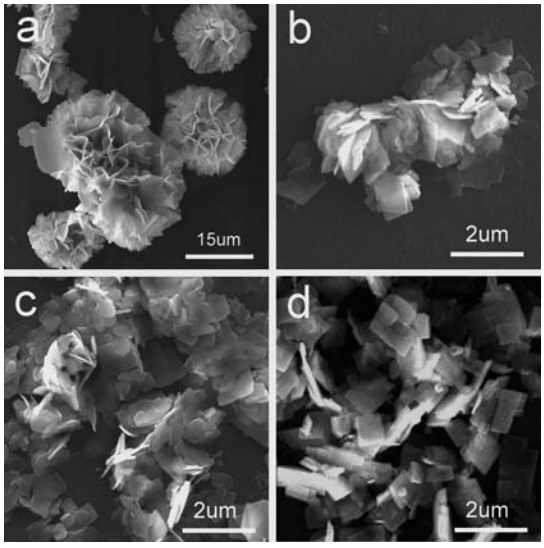

Figure 4. SEM images of the products obtained in a typical synthesis in the presence of different amounts of PVP: (a) 0.00 g, (b) 0.01 g, (c) 0.02 g, and (d) 0.04 g.

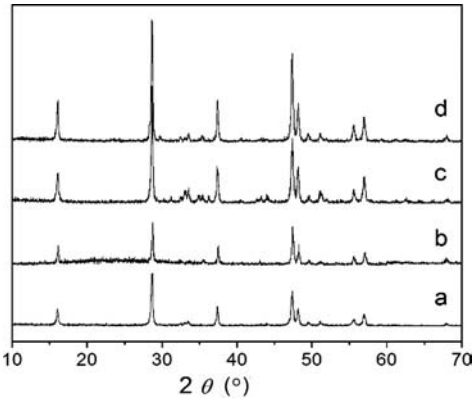

Figure 5. Powder XRD patterns of the products obtained in a typical synthesis with the addition of extra PVP. (a) 0.00 g, (b) 0.01 g, (c) 0.02 g, and (d) 0.04 g.

The Role of Solvent: the Control of Phase

Our previous work demonstrated that organic diol solvent has a great effect on the synthesis of $FeSe_x$.[28] We have successfully isolated pure-phase tetragonal $FeSe_x$ by adopting glycol as the solvent. In addition, we explored other polyols, such as 1,2-propanediol, 1,4-butanediol, and glycerol, as the solvent to prepare PbO-type $FeSe_x$. Instead of glycol, when 1,2-propanediol was used as solvent, the product identified by powder XRD pattern was phase-pure $FeSe_x$ (Figure 6a, 1#). The shape of the products was also platelike (Figure 6b). However, when either 1,4-butanediol or glycerol was applied as the solvent, diffraction peaks from the PbO-type phase could not be detected (Figure 6a, either 2# or 3#). SEM images of these products with different shapes were observed and are depicted in Figure 6c and d. These results suggest that phase-pure PbO-type $FeSe_x$ nanoplates can only be grown in the diol solvent with very short linear carbon chains, such as glycol and 1,2-propanediol, under our current experimental conditions. This implies a low possibility of harvesting phase-pure β-FeSe by using a simple solvent route. This may be because the structure of β-FeSe is not stable enough,[22] and Fe_3O_4 is easily formed even though the experiment was executed by standard oxygen-free techniques.[7] It was previously shown that the chemical composition and the edge length of the single crystalline $FeSe_x$ nanoflakes can be tailored readily by 1,2-tetradecanediol,[28] which serves as a reducing agent that facilitates the reduction of Se to Se^{2-} for the formation

of $FeSe_x$. Li and co-authors proposed that SeO_3^{2-} anions can be reduced by 1,2-PG to Se in alkali solution.[18] They also found that only amorphous Se could be obtained if the reaction rate was lowered or the aging time was shortened. Therefore, it can be believed that the reducing ability of the used solvent is very important for the formation of β-$FeSe_x$ with a proper proportion of Se and Fe from the reaction system. β-FeSe could not be obtained with 1,4-butanediol, probably because of the low reducing ability. However, when glycerol was used as the solvent, the pXRD of the product shows the presence of the Fe_3O_4 phase (Figure 6a, 3#). During the experiment, it was found that magnetic stirring was difficult because of the extremely strong viscidity of glycerol. It is easily acceptable that Se^{2-} and Fe^{2+} would be difficult to transfer and combine for the growth of β-FeSe. Thus, the viscidity of glycerol is the key handicap for the formation of β-FeSe. Therefore, it is considerably important to adopt an appropriate solvent for the successful growth of phase-pure PbO-type $FeSe_x$ nanoplates.

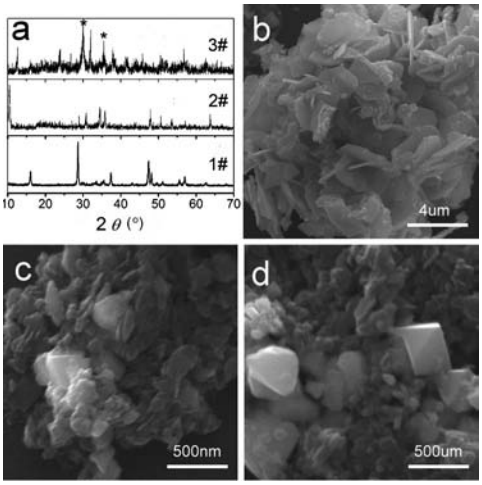

Figure 6. (a) Powder X-ray diffraction patterns and (b)–(d) SEM images of the products obtained from the solvent of (1#, b) 1,2-propanediol, (2#, c) 1,4-butanediol, and (3#, d) glycerol (*-Fe_3O_4), respectively.

Conclusions

In summary, PbO-type, tetragonal, nearly stoichiometric $FeSe_x$ (i.e. $x = 1.0$) nanoplates enclosed by (001) lattice planes as larger top-bottom surfaces and {100} as side surfaces have been grown through a facile solvothermal route in glycol from simple inorganic sources, i.e. $FeCl_2$ and Se powders. When the amount of PVP is increased, square nanoflakes become more apparent and more dispersed. In addition, the correct choice of a diol with short linear carbon chain as solvent is crucially important to facilitate phase-pure PbO-type tetragonal $FeSe_x$, whereas phase-pure tetragonal $FeSe_x$ could not be isolated when either 1,4-butanediol or glycerol was used as solvent. The facile and mild solvent method could be a promising new approach for the successful synthesis of phase-pure and well-dispersed $FeSe_x$ nanoplates.

Experimental Section

Synthesis: Iron chloride ($FeCl_2$ Guangdong Guanghua Chemical Co.), Se powders (Guangdong Guanghua Chemical Co.), glycol (Tianjin Fuyu Chemical Co.), sodium hydroxide pellets (NaOH, Guangdong Guanghua Chemical Co.), and polyvinyl pyrrolidone (PVP) all in A.R. grade were used as the starting materials without further purification. In a typical synthesis, tetragonal β-$FeSe_x$ nanoplates, $FeCl_2$ (0.063 g, 0.5 mmol), Se powder (0.040 g, 0.5 mmol), NaOH (0.120 g, 3.0 mmol), and PVP (0.030 g) were dissolved under vigorous magnetic stirring in glycol (10.0 mL) for 2.0 h. The mixture was sealed in a Teflon-lined stainless steel autoclave (25 mL) and maintained at 220 °C for 12 h for solvothermal crystallization. Followed by natural cooling to ambient temperature, the resulting solid products were washed with distilled water (10 mL), then absolute ethanol (10 mL) by centrifugation (two times). The as-obtained black samples were dried in vacuo at room temperature.

Characterization: The products were characterized by powder X-ray diffraction (pXRD), scanning electron microscopy (SEM), transmission electron microscopy (TEM), and high-resolution TEM (HRTEM). XRD patterns were recorded with a Rigaku D/MAX 2200 VPC diffractometer by using Cu-K_α radiation (λ = 0.15045 nm) and a graphite monochromator. SEM images were taken with FEI Quanta 400 Thermal FE Environment Scanning Electron Microscope. Samples were gold-coated prior to SEM analysis. TEM images were prepared on a JEM-2010HR transmission electron microscope operated at an accelerating voltage of 200 kV. The microscope was equipped with a Oxford EDS spectrometer and Gatan GIF Tridiem systems for both structural and chemical analysis. TEM samples were prepared by dispersing the powders on holey carbon film supported on copper grids. The elemental analysis of the as-prepared β-FeSe sample was carried out by using inductively coupled plasma atomic emission spectrometry (ICP-AES) on TJA IRIS (HR).

Acknowledgments

This work was supported financially by the National Natural Science Foundation of China (NSFC) and the Government of Guangdong Province for National Science Foundation (NSF) (Grants U0734002, 50872158, and 8251027501000010). Part of the synthesis was conducted at SUNY Binghamton and supported by NSF DMR-0731382. M. M. W. and L. Q. C. greatly appreciate the help provided by Prof. Jiye (James) Fang, in the Department of Chemistry, State University of New York at Binghamton.

[1] Q. J. Feng, D. Z. Shen, J. Y. Zhang, B. S. Li, B. H. Li, Y. M. Lu, X. W. Fan, H. W. Liang, *Appl. Phys. Lett.* **2006**, *88*, 012505.
[2] K. W. Liu, J. Y. Zhang, D. Z. Shen, C. X. Shan, B. H. Li, Y. M. Lu, X. W. Fan, *Appl. Phys. Lett.* **2007**, *90*, 262503.
[3] X. J. Wu, Z. Z. Zhang, J. Y. Zhang, Z. G. Ju, B. H. Li, B. S. Li, C. X. Shan, D. X. Zhao, B. Yao, D. Z. Shen, *Thin Solid Films* **2008**, *516*, 6116–6119.
[4] M. Z. Xue, Z. W. Fu, *Acta Chim. Sinica* **2007**, *65*, 2715–2719.
[5] X. J. Wu, D. Z. Shen, Z. Z. Zhang, J. Y. Zhang, K. W. Liu, B. H. Li, Y. M. Lu, B. Yao, D. X. Zhao, B. S. Li, C. X. Shan, X. W. Fan, H. J. Liu, C. L. Yang, *Appl. Phys. Lett.* **2007**, *90*, 112105.
[6] X. J. Wu, Z. Z. Zhang, J. Y. Zhang, Z. G. Ju, D. Z. Shen, B. H. Li, C. X. Shan, Y. M. Lu, *J. Cryst. Growth* **2007**, *300*, 483–485.
[7] F. C. Hsu, J. Y. Luo, K. W. Yeh, T. K. Chen, T. W. Huang, P. M. Wu, Y. C. Lee, Y. L. Huang, Y. Y. Chu, D. C. Yan, M. K. Wu, *Proc. Natl. Acad. Sci. USA* **2008**, *105*, 14262–14264.

[8] H. Kotegawa, S. Masaki, Y. Awai, H. Tou, Y. Mizuguchi, Y. Takano, *J. Phys. Soc. Jpn.* **2008**, *77*, 113703.
[9] Y. Mizuguchi, F. Tomioka, S. Tsuda, T. Yamaguchi, Y. Takano, *Appl. Phys. Lett.* **2008**, *93*, 152505.
[10] D. Braithwaite, B. Salce, G. Lapertot, F. Bourdarot, C. Marin, D. Aoki, M. Hanfland, *J. Phys. Condens. Matter* **2009**, *21*, 232202.
[11] L. Li, Z. R. Yang, M. Ge, L. Pi, J. T. Xu, B. S. Wang, Y. P. Sun, Y. H. Zhang, *J. Supercond. Novel Magn.* **2009**, *22*, 667–670.
[12] S. Margadonna, Y. Takabayashi, Y. Ohishi, Y. Mizuguchi, Y. Takano, T. Kagayama, T. Nakagawa, M. Takata, K. Prassides, *Phys. Rev. B* **2009**, *80*, 064506.
[13] J. N. Millican, D. Phelan, E. L. Thomas, J. B. Leao, E. Carpenter, *Solid State Commun.* **2009**, *149*, 707–710.
[14] V. A. Sidorov, A. V. Tsvyashchenko, R. A. Sadykov, *J. Phys. Condens. Matter* **2009**, *21*, 415701.
[15] M. J. Wang, J. Y. Luo, T. W. Huang, H. H. Chang, T. K. Chen, F. C. Hsu, C. T. Wu, P. M. Wu, A. M. Chang, M. K. Wu, *Phys. Rev. Lett.* **2009**, *103*, 117002.
[16] T. Hanaguri, S. Niitaka, K. Kuroki, H. Takagi, *Science* **2010**, *328*, 474–476.
[17] K. D. Oyler, X. L. Ke, I. T. Sines, P. Schiffer, R. E. Schaak, *Chem. Mater.* **2009**, *21*, 3655–3661.
[18] M. L. Li, Q. Z. Yao, G. T. Zhou, S. Q. Fu, *CrystEngComm* **2010**, *12*, 3138–3144.
[19] T. M. McQueen, Q. Huang, V. Ksenofontov, C. Felser, Q. Xu, H. Zandbergen, Y. S. Hor, J. Allred, A. J. Williams, D. Qu, J. Checkelsky, N. P. Ong, R. J. Cava, *Phys. Rev. B* **2009**, *79*, 014522.
[20] A. J. Williams, T. M. McQueen, R. J. Cava, *Solid State Commun.* **2009**, *149*, 1507–1509.
[21] B. C. Sales, A. S. Sefat, M. A. McGuire, R. Y. Jin, D. Mandrus, Y. Mozharivskyj, *Phys. Rev. B* **2009**, *79*, 094521.
[22] B. H. Mok, S. M. Rao, M. C. Ling, K. J. Wang, C. T. Ke, P. M. Wu, C. L. Chen, F. C. Hsu, T. W. Huang, J. Y. Luo, D. C. Yan, K. W. Ye, T. B. Wu, A. M. Chang, M. K. Wu, *Cryst. Growth Des.* **2009**, *9*, 3260–3264.
[23] S. B. Zhang, X. D. Zhu, H. C. Lei, G. Li, B. S. Wang, L. J. Li, X. B. Zhu, Z. R. Yang, W. H. Song, J. M. Dai, Y. P. Sun, *Supercond. Sci. Technol.* **2009**, *22*, 075016.
[24] U. Patel, J. Hua, S. H. Yu, S. Avci, Z. L. Xiao, H. Claus, J. Schlueter, V. V. Vlasko-Vlasov, U. Welp, W. K. Kwok, *Appl. Phys. Lett.* **2009**, *94*, 082508.
[25] V. P. Swati, G. P. Vilas, G. Aharon, *J. Phys. Chem. C* **2007**, *111*, 16781–16786.
[26] Y. J. Xia, F. Q. Huang, X. M. Xie, M. H. Jiang, *Europhys. Lett.* **2009**, *86*, 37008.
[27] A. P. Liu, X. Y. Chen, Z. J. Zhang, Y. Jiang, C. W. Shi, *Solid State Commun.* **2006**, *138*, 538.
[28] L. Q. Chen, H. Q. Zhan, X. F. Yang, Z. Y. Sun, J. Zhang, D. Xu, C. L. Liang, M. M. Wu, J. Y. Fang, *CrystEngComm* **2010**, *12*, 4386–4391.
[29] Y. J. Sun, B. Mayers, T. Herricks, Y. N. Xia, *Nano Lett.* **2003**, *3*, 955–960.
[30] Y. Wang, J. Chen, L. Chen, Y. B. Chen, L. M. Wu, *Cryst. Growth Des.* **2010**, *10*, 1578–1584.
[31] F. Bonet, K. Tekaia-Elhsissen, K. V. Sarathy, *Bull. Mater. Sci.* **2000**, *23*,165–168.
[32] J. Zeng, X. H. Xia, M. Rycenga, P. Henneghan, Q. G. Li, Y. N. Xia, *Angew. Chem. Int. Ed.* **2010**, *49*, 1–6.

Received: December 8, 2010
Published Online: March 18, 2011

